Eur. Phys. J. A **25**, s01, 527–529 (2005)
DOI: 10.1140/epjad/i2005-06-052-x

EPJ A direct
electronic only

Unrestricted TDHF studies of nuclear response in the continuum

T. Nakatsukasa[a] and K. Yabana

Center for Computational Science and Institute of Physics, University of Tsukuba, Tsukuba 305-8571, Japan

Received: 7 October 2004 /
Published online: 6 May 2005 –

Abstract. The TDHF dynamics in the small-amplitude regime is studied in the real-space and real-time representation. The continuum is taken into account by introducing a suitable complex potential. This is equivalent to the continuum random-phase approximation and applicable to deformed nuclei.

PACS. 21.60.Jz Hartree-Fock and random-phase approximations – 24.30.Cz Giant resonances

1 Introduction

The time-dependent Hartree-Fock (TDHF) theory is a dynamical theory and takes care of both collective and single-particle excitations. Its small-amplitude regime is known as the random-phase approximation (RPA) for the effective density-dependent forces. The spreading width, which is partially described in the TDHF (one-body dissipation), is known to be important for the broadening of giant resonances. However, for light nuclei, the escape width gives a dominant contribution and becomes even more important near the drip line. Recently, we have proposed a feasible method to treat the continuum in the real-space TDHF calculation [1,2,3]. That is the absorbing-boundary condition (ABC) approach. We studied photoabsorption in molecules [4] and nuclear breakup reaction [5,6] with the similar technique.

The method, we call TDHF + ABC, is simple and accurate enough to calculate nuclear response in the continuum for spherical and deformed nuclei. Its small amplitude limit is equivalent to the continuum RPA [7]. An advantage over the continuum RPA is its applicability to non-spherical systems. In addition, the TDHF wave function in the coordinate space provides us with an intuitive picture of nuclear collective motion and the damping mechanism of particle escaping. The time evolution of the TDHF states is calculated following the prescription in ref. [8]. The trick to treat the continuum is introduction of an absorbing complex potential outside of the interacting region. The potential must be properly chosen so as to make the minimum reflection. We would like readers to refer to our recent paper [3] for computational details.

2 Octupole states in ^{16}O

In this section, we discuss the isoscalar octupole resonances in ^{16}O with the simple BKN interaction. A perturbative external field is chosen as $V_{\rm ext}(\mathbf{r}) = r^3 Y_{30}$. The time evolution is determined by the TDHF equation with the complex absorbing potential, $-i\eta(\mathbf{r})$,

$$i\hbar\frac{\partial}{\partial t}\psi_i(\mathbf{r},t) = \{h[\rho] + \epsilon V_{\rm ext}(\mathbf{r})\delta(t) - i\eta(\mathbf{r})\}\,\psi_i(\mathbf{r},t), \quad (1)$$

where $i = 1, \cdots, A/4$ and ϵ is a small parameter to validate the linear response approximation. The BKN interaction assumes the exact spin-isospin symmetry, thus each orbital has a four-fold degeneracy. $\eta(\mathbf{r})$ is zero in the physically relevant region of space. The single-particle wave functions are represented on the three-dimensional coordinate space. See ref. [3] for details.

The time evolution of the density calculated with and without the ABC is shown in fig. 1. The horizontal axis is z-axis. There is no difference up to $t < 0.8$ $\hbar$/MeV between the box (left panel) and absorbing boundary condition (right). However, the waves reflected at the edge of the space return to the nucleus for $t > 1$ $\hbar$/MeV (left). As a result, the time-dependent octupole moment shows a beating pattern created by the reflected waves. The reflection is a consequence of the discretized continuum in the energy representation.

In fig. 1, we can also see that, the octupole resonance emits particles along the z-axis and to the diagonal direction. This can be understood in terms of the pear shape of Y_{30} mode. In the numerical calculation, we stop the time evolution at $t = 30$ $\hbar$/MeV. The Fourier transform of the time-dependent octupole moment leads to the octupole strength function in fig. 2. We use a smoothing parameter $\Gamma = 0.2$ MeV to make low-energy peaks below the particle threshold with a finite width. The octupole oscillation with $E = 11.3$ MeV is stable with respect to the particle decay. On the other hand, the high-energy resonance is in the continuum. The particle escape almost ceases by $t = 1$ $\hbar$/MeV and only a low-frequency octupole oscillation survives after that (fig. 1). Taking into account the particle continuum properly, the high-frequency octupole

[a] Conference presenter;
e-mail: takashi@nucl.ph.tsukuba.ac.jp

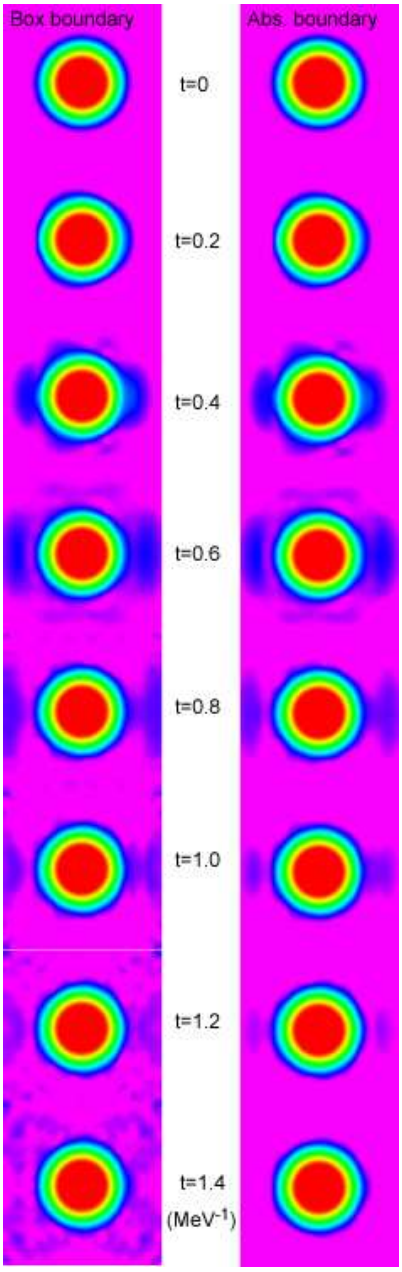

Fig. 1. Density plots in the zx plane in the logarithmic scale. The times t is given in units of $\hbar$/MeV. The box boundary condition is used in the left panel, while the ABC is applied in the right one.

resonance is significantly broadened by the particle escape. Note that the peak at $E \approx 2.5$ MeV is due to small admixture of the translational mode.

3 Low-energy dipole states in Be isotopes

We study $E1$ responses in neutron-rich Be isotopes using the same technique as in sect. 2. The full Skyrme functional (SIII) is used in the calculation. The TDHF equation, eq. (1), is solved with the $E1$ external field for

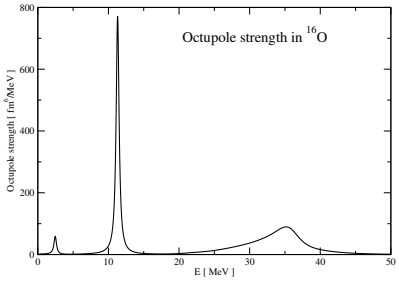

Fig. 2. Isoscalar octupole strength for ^{16}O as a function of excitation energy, being calculated with the ABC.

$V_{\rm ext}(\mathbf{r})$. See ref. [3] for full details. For ^{12}Be, we obtain the ground state with a small prolate deformation. The lowest dipole state appears near the threshold, at $E \approx 4.5$ MeV, with $B(E1; 0^+ \to 1^-) = 0.023$ e^2 fm^2. The corresponding experimental data [9] indicate $E = 2.68$ MeV with $B(E1) = 0.051(13)$ e^2 fm^2. Some experiments suggest that ^{12}Be has a large deformation in the ground state [10]. Since the ground-state deformation is very small in this calculation, this might be a reason of the discrepancy.

For ^{14}Be, the HF ground state has a superdeformed prolate shape ($\beta \approx 0.75$). The low-energy dipole state is embedded in the continuum at $E \approx 5$ MeV having a significant $E1$ strength, $B(E1) \approx 0.26$ e^2 fm^2. The peak position is almost at the same energy as that in ^{12}Be, however, the strength is about 10 times larger. Experiment seems to suggest some enhancement of Coulomb dissociation cross-section around $E \approx 2$ and ≈ 5 MeV [11].

4 Conclusion

We have studied nuclear response in the continuum for spherical and deformed nuclei. The absorbing boundary condition approach is utilized in the TDHF simulation in the small amplitude regime. This is equivalent to the continuum RPA, but easier to apply to deformed nuclei. In this paper, we have shown the application to octupole states in ^{16}O and dipole states in ^{12,14}Be. Strong enhancement of the $E1$ strength at the neutron drip line is obtained for ^{14}Be.

This work is supported by the Grant-in-Aid for Scientific Research in Japan (Nos. 14540369 and 14740146).

References

1. T. Nakatsukasa, K. Yabana, Prog. Theor. Phys. Suppl. **146**, 447 (2002).
2. T. Nakatsukasa, K. Yabana, Eur. Phys. J. A **20**, 163 (2004).
3. T. Nakatsukasa, K. Yabana, Phys. Rev. C **71**, 024301 (2005).
4. T. Nakatsukasa, K. Yabana, J. Chem. Phys. **114**, 2550 (2001).

5. M. Ueda, K. Yabana, T. Nakatsukasa, Phys. Rev. C **67**, 014606 (2002).
6. M. Ueda, K. Yabana, T. Nakatsukasa, Nucl. Phys. A **738**, 288 (2004).
7. S. Shlomo, G.F. Bertsch, Nucl. Phys. A **243**, 507 (1975).
8. H. Flocard, S.E. Koonin, M.S. Weiss, Phys. Rev. C **17**, 1682 (1978).
9. H. Iwasaki *et al.*, Phys. Lett. B **491**, 8 (2000).
10. A. Navin *et al.*, Phys. Rev. Lett., **85**, 266 (2000).
11. M. Labiche *et al.*, Phys. Rev. Lett. **86**, 600 (2001).